Acoustic Velocities and Phase Transitions in Molybdenum under Strong Shock Compression

R. S. Hixson, D. A. Boness,[a] and J. W. Shaner
Los Alamos National Laboratory, University of California, Los Alamos, New Mexico 87545

J. A. Moriarty
Lawrence Livermore National Laboratory, University of California, Livermore, California 94550
(Received 4 November 1988)

We present acoustic velocity data that demonstrate a high-pressure solid-solid phase transition in molybdenum at about 2.1 Mbar and 4100 K. This observation is supported here by first-principles theoretical calculations which predict a zero-temperature bcc → hcp transition within our experimental pressure range. In addition, our results show the melting transition for shock-compressed Mo at about 3.9 Mbar and 10000 K.

PACS numbers: 64.30.+t, 62.50.+p

The idea that structural phase stability in transition and rare-earth metals is controlled by the number of valence d electrons per atom, Z_d, has gained widespread acceptance in recent years and is now well supported by detailed quantum-mechanical calculations.[1] In the case of the carefully studied rare earths, Z_d is found to increase both with *decreasing* atomic number through the series and with increased density for a given element, such that for either variation the same sequence of structures is obtained, in agreement with experiment.[2] In transition metals, on the other hand, Z_d can be increased by *increasing* atomic number, alloying with an element of higher Z_d, or, in principle, by transferring electrons from s- and p-like states to d-like states with compression (the so-called $s \rightarrow d$ transition[3]). The atomic number effect explains the canonical hcp-bcc-hcp-fcc sequence of structures observed across the nonmagnetic $4d$ and $5d$ transition series and is responsible for the extreme stability of the bcc structure in Mo and W compared with the stable hcp structure of Tc and Re. Although there has been speculation on a high-pressure bcc → hcp transition in Mo based on empirical alloy data,[4] heretofore no pressure-induced phase transitions have even been observed in the nonmagnetic transition metals to the right of the group-IVB elements Ti, Zr, and Hf. In this Letter we present the first direct experimental and theoretical evidence for such a transition in Mo.

The absence of previously observed phase transitions in the central transition metals partly reflects the difficulty in making such measurements at the multimegabar pressures needed to drive the $s \rightarrow d$ transition in these materials. While conventional shock-wave techniques can reach the required pressure regime, the volume changes occurring for either solid-solid transitions or melting are usually too small to be seen in the pressure-volume data recorded, and in Mo at high-pressure Hugoniot points are very scarce. Acoustic velocity, on the other hand, is a derivative quantity of the equation-of-state surface of a material and is more sensitive to changes in structural properties than pressure or volume. Consequently, measurement of the sound velocity during shock compression can be used as a sensitive probe for detecting phase transitions. Moreover, when sound velocities are combined with other measured quantities—pressure, density, and temperature—it is possible to calculate additional derivative properties such as the Grüneisen parameter, specific heats, and bulk moduli.

To measure the acoustic velocity in compressed Mo, we have used a shock and rarefaction overtake method described in detail elsewhere.[5] The velocity of a pressure-release wave (rarefaction) following a strong shock is measured by observing the point at which it overtakes the shock front. To generate the shock we hit a target with a thin (~1 mm) flyer plate accelerated in a two-stage light-gas gun to velocities up to 7.6 km/s. After impact, a shock propagates forward in the target and backward in the flyer. The shock is reflected as a forward-moving rarefaction wave at the rear surface of the flyer. Because this rarefaction is moving into hot dense material, it can overtake the forward-moving shock and reduce the shock front pressure and temperature, and this may easily be observed.

The Mo target has four steps of different thickness shown in Fig. 1. Behind these steps is a brass cell filled with bromoform, the analyzer material. When shock compressed, the bromoform is a very efficient emitter of thermal radiation, the intensity of which can be mea-

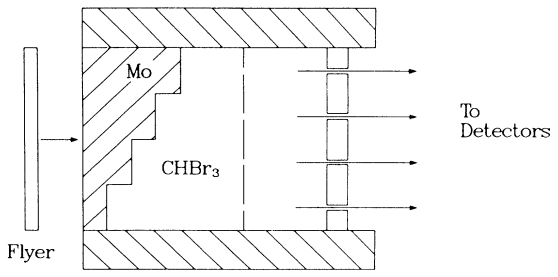

FIG. 1. Schematic of the target assembly.

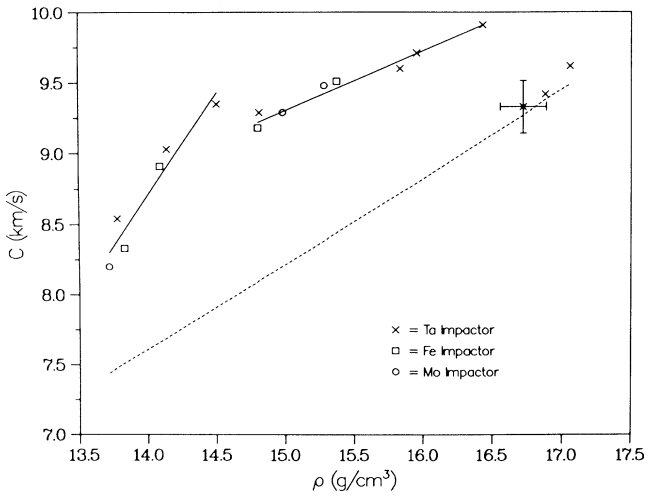

FIG. 2. Sound velocity in molybdenum plotted against density on the Hugoniot curve. Solid lines are linear fits to data; the dotted curve is the calculated bulk sound velocity assuming the shock parameters of Table I and the approximation $\rho\gamma_G$ =const.

sured as a function of time. The target and flyer thicknesses are fixed so that the overtake occurs in the bromoform in each case. The four target thicknesses allow the effects of the Mo-bromoform interface to be eliminated by simply extrapolating the overtake distances and times to a larger thickness. The corresponding overtake distance, D_{ovt}, represents the thickness of target material at which the rarefaction would overtake the shock at the Mo-bromoform interface.

The sound velocity in the shock-compressed material is the velocity of the leading edge of the rarefaction wave. For an impact of an Mo flyer on an Mo target, this sound velocity can be calculated from[5]

$$C = U_S(\rho_0/\rho)[(R+1)/(R-1)], \quad (1)$$

where R is the ratio of D_{ovt} to flyer thickness, and U_S and ρ are the shock velocity and density behind the shock, respectively. For this symmetric impact the particle velocity behind the shock is exactly one-half the measured flyer velocity, and the shock parameters can be calculated from the known Hugoniot curve for Mo.[6] The Hugoniot curve for Mo has been taken as a fit to previously measured data points. We have also used iron and tantalum flyers, both of which have been well characterized for both shock and release properties.[7-8] The more complicated calculation for these unsymmetrical impacts is given elsewhere.[9]

The experimental technique described here measures only the velocity of the beginning of the release wave. In a solid this velocity will be that of a longitudinal elastic wave ($C = C_L$), while for a partially molten material it is that of a bulk wave ($C = C_B$). The transition in wave velocity from longitudinal to bulk defines the point at which the Hugoniot curve crosses the solidus.[8,10]

The acoustic velocity measurements in shock-compressed Mo are shown in Fig. 2 and listed in Table I. We have plotted the acoustic velocity versus density because data from many other metals have shown a roughly linear relationship over large density ranges.[8,11-13] The most important features of Fig. 2 are the breaks occurring at 14.5 and 16.5 g/cm^3, as these are associated

TABLE I. Molybdenum shock data. Hugoniot equations are as follows: (1) iron (Ref. 10): $U_S = 1.58U_P + 3.955$, $\rho_0 = 7.85$ g/cm^3; (2) molybdenum (Ref. 6): $U_S = 1.255U_P + 5.143$, $\rho_0 = 10.206$ g/cm^3; (3) tantalum (Ref. 7): $U_S = 1.307U_P + 3.293$, $\rho_0 = 16.67$ g/cm^3, where U_S is shock velocity in km/s, U_P is particle velocity in km/s, and ρ_0 is initial density.

ρ (g/cm^3)	U_{proj} (km/s)	Flyer	P (Mbar)	C (km/s)	C_B (km/s)	γ_G
13.72	3.89	Mo	1.50	8.20	7.44	···
13.78	3.66	Ta	1.54	8.54	7.48	···
13.83	4.52	Fe	1.57	8.33	7.51	···
14.09	4.85	Fe	1.74	8.91	7.66	···
14.14	4.06	Ta	1.78	9.03	7.69	···
14.50	4.46	Ta	2.03	9.35	7.91	···
14.80	5.80	Fe	2.25	9.18	8.09	···
14.81	4.82	Ta	2.26	9.29	8.10	···
14.98	5.46	Mo	2.39	9.29	8.20	···
15.28	5.86	Mo	2.64	9.48	8.38	···
15.37	6.57	Fe	2.71	9.51	8.44	···
15.83	6.03	Ta	3.13	9.60	8.72	···
15.95	6.17	Ta	3.23	9.71	8.79	···
16.43	6.78	Ta	3.72	9.91	9.09	···
16.72	7.14	Ta	4.02	9.33	9.27	0.99
16.88	7.36	Ta	4.21	9.42	9.38	1.00
17.06	7.58	Ta	4.41	9.62	9.49	0.92

with changes in the properties of shock-compressed Mo which have not been observed previously. In Table I we give the Hugoniot parameters used in all calculations, as well as the data points. Typical uncertainties are $\pm 2\%$ in sound velocity and $\pm 1\%$ in density.

The break in the sound velocity data above 16.5 g/cm^3 (3.9 Mbar) can be attributed to melting, as previously observed in Fe,[8] for example. To calculate the bulk sound velocity, C_B, shown in Fig. 2 and listed in Table I, we have used the common assumption that $\rho\gamma_G$ is constant[14] where γ_G is the Grüneisen parameter and the relation[15]

$$\gamma_G = 2\frac{B_S - B_H}{P_H - \eta(V_0/V)B_H} . \quad (2)$$

In Eq. (2), B_S and B_H are the bulk moduli defined along an isentrope and the Hugoniot curve, respectively, and $\eta = 1 - V/V_0$. Equation (2) allows one to calculate γ_G from the bulk sound velocity, $C_B = (B_S/\rho)^{1/2}$, and the Hugoniot point, or, by inversion, C_B from the Hugoniot parameters and a model for γ_G. The agreement between the model calculation and the data above 16.5 g/cm^3 shows that the Mo is partially molten at the highest pressures.

The first break in the sound velocity curve above 14.5 g/cm^3 (2.1 Mbar), on the other hand, can be attributed to a change in elastic properties associated with a solid-solid phase change. This phenomenon has been observed previously in the solid-solid $\epsilon \rightarrow \gamma$ phase transformation in iron.[8] Since the longitudinal elastic wave velocity is related to the bulk wave velocity through

$$C_L = C_B \left[\frac{3(1-\nu)}{(1+\nu)} \right]^{1/2} , \quad (3)$$

where ν is Poisson's ratio, any change in solid phase which changes ν will be seen in these experiments. The data between 14.5 and 16.5 g/cm^3 are consistent with a Poisson's ratio of 0.4, which is significantly higher than the normal-density value of 0.26 for bcc Mo. However, under shock conditions the microstructure of the new phase is unknown.

In order to see if there is a basis for expecting solid-solid phase transitions in Mo, we have studied theoretically the electronic structure and energetics of this material within the framework of the Kohn-Sham local-density formalism,[16] utilizing the first-principles linear-muffin-tin-orbital method.[17,18] Specifically, zero-temperature total energies, $E_0(V)$, and pressures, $P_0(V)$, have been calculated for the bcc structure over the volume range $0.4 < V/V_0 < 1.1$. In addition, bcc-fcc and hcp-fcc energy differences have been obtained by means of the Andersen force theorem.[19] These latter results are illustrated in Fig. 3 and show both that the observed bcc structure correctly has the lowest total energy near $V = V_0$, and that below $V = 0.8V_0$ this structure is rapidly destabilized. A bcc $\rightarrow$ hcp $\rightarrow$ fcc sequence of phase

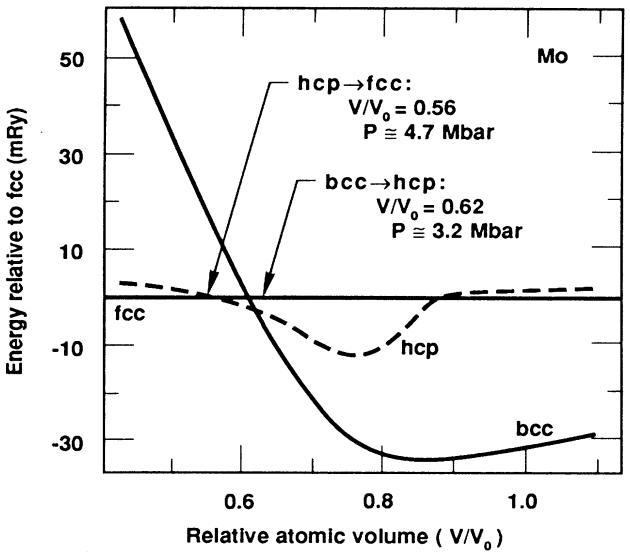

FIG. 3. Theoretical bcc-fcc and hcp-fcc total-energy differences at zero temperature as a function of volume in molybdenum.

transitions is predicted, with the first transition occurring at about 16.5 g/cm^3 (3.2 Mbar). These structural phase transitions are driven by a continuous $s \rightarrow d$ transfer of electrons into the $4d$ electron energy bands with decreasing volume. We tentatively identify the bcc $\rightarrow$ hcp transition with the solid-solid transition observed in the present experiments, although as yet we have not ruled out the possibility of an intermediate (distorted or low-symmetry) phase appearing before hcp, which would lower the theoretical transition pressure. Also, we have not considered the effects of phonons and high temperature on the phase stability, which may bring theory and experiment into better agreement. To address these complications, one needs both central and angular forces in molybdenum, and these are currently under development.[20] We have, however, made a simple calculation of the Grüneisen-parameter function $\gamma_G(V)$ based on the volume derivatives of P_0.[21] Consistent with normal-density thermodynamic data, we find $\gamma_G = 1.7$ at $V = V_0$, and consistent with the present experimental results, we find $\gamma_G = 0.95$ at the observed onset of melting. From $P_0(V)$ and $\gamma_G(V)$ we have further calculated a Hugoniot curve, $P_H(V)$, which is in excellent agreement with established shock-wave data.[6] The estimated temperatures T_H at the locations of the present observed phase transitions are 4100 K near the solid-solid transition and 10000 K around melting. By comparison, the Lindemann melting law,

$$\frac{d\ln T_m}{d\ln\rho} = 2\gamma_G(\rho) - 2/3 , \quad (4)$$

with $\rho\gamma_G$ constant predicts a melting temperature, T_m, of 9300 K at a density of 16.5 g/cm^3.

Our electronic structure calculations further show that an increase in $4d$ occupation number Z_d of roughly 0.5 electron per atom is needed to drive the bcc → hcp phase transition in Mo with pressure. The same conclusion is reached if instead one increases Z_d by continuously increasing atomic number in the $4d$ transition series, as can be seen from Fig. 11 of Ref. 1. To see the equivalent effect of alloying, one may compare the experimental phase diagrams of the Mo-Tc, Mo-Ru, Mo-Rh, and Mo-Pd systems.[22] The bcc, Mo-rich, components of the eutectics have maximum solute concentrations of 50%, 30%, 20%, and 10%, respectively. Ignoring the screening of the solute, these systems all have roughly 6.5 valence electrons per atom at maximum solute concentration, or roughly 0.5 electron higher than pure Mo. A similar relation applies for the alloy sequence W-Re, W-Os, W-Ir, and W-Pt. Thus an increase of approximately 0.5 d electron per atom appears to destabilize the bcc structure of the group-VIB transition metals. We expect, therefore, that high-pressure solid-solid phase transitions analogous to that observed here for Mo should also exist for Cr and W.

We wish to thank C. Swenson, D. Shampine, and T. Rust for their help in making the measurements and B. Olinger and J. Fritz for useful discussions. This work is presented under the auspices of the United States Department of Energy.

[a]Present address: Department of Physics, Santa Clara Univeristy, Santa Clara, CA 95053.

[1]H. L. Skriver, Phys. Rev. B **31**, 1909 (1985), and references therein.

[2]U. Benedict, W. A. Grosshans, and W. B. Holzapfel, Physica (Amsterdam) **244B**, 14 (1986).

[3]A. K. McMahan, Physica (Amsterdam) **139&140B**, 31 (1986).

[4]V. A. Zil'bershteyn, L. B. Zaretskiy, and E. I. Estrin, Fiz. Met. Metalloved. **40**, 587 (1975).

[5]R. G. McQueen, J. W. Hopson, and J. N. Fritz, Rev. Sci. Instrum. **53**, 245 (1982).

[6]LLL Report No. UCRL-50108, 1977, edited by M. van Thiel, J. Shaner, and E. Salinas (unpublished), Vol. 1.

[7]A. C. Mitchell and W. Nellis, J. Appl. Phys. **52**, 3363 (1981).

[8]J. M. Brown and R. G. McQueen, J. Geophys. Res. **91**, 7485 (1986).

[9]R. G. McQueen, J. N. Fritz, and C. E. Morris, in *Shock Waves in Condensed Matter-1983,* edited by J. R. Assay, R. A. Graham, and G. K. Straub (North-Holland, Amsterdam, 1984), p. 95.

[10]J. R. Asay, J. Appl. Phys. **48**, 2832 (1977).

[11]D. A. Boness, J. M. Brown, and J. W. Shaner, in *Shock Waves in Condensed Matter-1987,* edited by S. C. Schmidt and N. Holmes (North-Holland, Amsterdam, 1988), p. 115.

[12]R. S. Hixson, M. A. Winkler, and J. W. Shaner, High Temp. High Pressure **18**, 635 (1986).

[13]R. S. Hixson, M. A. Winkler, and J. W. Shaner, Physica (Amsterdam) **139&140B**, 893 (1986).

[14]R. G. McQueen, S. P. Marsh, J. W. Taylor, J. N. Fritz, and W. J. Carter, in *High Velocity Impact Phenomena,* edited by R. Kinslow (Academic, New York, 1970).

[15]C. A. Swenson, J. W. Shaner, and J. M. Brown, Phys. Rev. B **34**, 7924 (1986).

[16]W. Kohn and L. J. Sham, Phys. Rev. **140**, A1133 (1965); L. Hedin and B. I. Lundqvist, J. Phys. C **4**, 2064 (1971).

[17]*The LMTO Method,* edited by H. L. Skriver, Spinger Series in Solid State Sciences Vol. 41 (Springer-Verlag, Berlin, 1984).

[18]The present self-consistent LMTO calculations employ the atomic-sphere approximation, the combined-correction term to this approximation, and s, p, d, and f angular momentum components in a nonrelativistic mode.

[19]A. R. Mackintosh and O. K. Andersen, in *Electrons at the Fermi Surface,* edited by M. Springford (Cambridge Univ. Press, Cambridge, 1980).

[20]J. A. Moriarty, Phys. Rev. B **38**, 3199 (1988), and unpublished.

[21]We have used the well known formula of J. S. Dugdale and D. K. C. McDonald, Phys. Rev. **89**, 832 (1953).

[22]*Binary Alloy Phase Diagrams,* edited by T. B. Massalski (American Society for Metals, Metals Park, Ohio, 1987), Vol. 2.